Journal of Supramolecular Structure 2:82–98 (1974)

THREE-DIMENSIONAL STRUCTURES AT 5.5 Å RESOLUTION AND REGULATORY PROCESSES IN ASPARTATE TRANSCARBAMYLASE FROM E. COLI

W. N. Lipscomb, D. R. Evans, B. F. P. Edwards, S. G. Warren, S. Pastra-Landis, and D. C. Wiley

Gibbs Chemical Laboratory, Harvard University, Cambridge, Massachusetts 02138

The three-dimensional structure of the multisubunit allosteric enzyme, aspartate transcarbamylase, has been determined to 5.5 Å resolution. An unusual feature of the molecule is a large central aqueous cavity 50 Å × 50 Å × 25 Å, into which the active sites face. Access to the central cavity and the active site region is provided by six equivalent channels of 15 Å diameter.

A complex C_6R_4, composed of catalytic trimers C_3 and of regulatory dimers R_2, has been isolated upon treatment of aspartate transcarbamylase (ATCase, C_6R_6) by mercurials. The specific catalytic activity of C_6R_4 is essentially the same as that of ATCase, about 70% of that of the catalytic trimers at 30 mM aspartate and saturating carbamyl phosphate. Allosteric interactions are reduced in C_6R_4 as compared with those in ATCase. In the homotropic interactions the Hill coefficient is reduced from approximately 3.3 to 2.1 at pH 8.3, while the heterotropic interactions of both cytidine triphosphate (CTP) and adenosine triphosphate (ATP) are reduced substantially but not abolished at pH 8.3. Thus, the allosteric transitions involved in the regulatory mechanisms do not require the intact structure C_6R_6. Also, this regulation is not simply the control of access of substrates or products to or from the large central aqueous cavity in the ATCase molecule.

Comparison of electron density maps at 5.5 Å resolution for ATCase and for the complex of ATCase with CTP shows substantial similarities throughout the three-dimensional electron density maps. Significant differences are seen, however, in the region of the regulatory dimers R_2 where CTP adds, and near the active sites in the catalytic trimers C_3.

Allosteric enzymes participate in one of the major control mechanisms which have evolved in living organisms for coordination of the myriad chemical reactions within cells. Many of these enzymes, like aspartate transcarbamylase (EC 2.1.3.2) of *E. coli*, catalyze

the first committed step of an important biochemical pathway. As a consequence of this strategic location, allosteric enzymes control the flow of metabolites through the pathway in response to requirements of the organism. It is generally believed that these enzymes undergo conformational changes that are induced by binding of effectors (allosteric inhibitors or activators) to specific sites distinct from the catalytic site. These conformational changes are transmitted through the molecule, altering the environment of the catalytic site. However, the detailed mechanisms of this fundamental process, essential for rapid and precise regulation of intracellular metabolism, are not understood.

Aspartate transcarbamylase (ATCase)* is an allosteric enzyme (1, 2) that catalyzes the first step in pryrimidine biosynthesis: the reaction of aspartate and carbamylphosphate to yield carbamylaspartate and phosphate (Fig. 1). The activity of ATCase is modulated by several allosteric effectors (Fig. 2). Cytidine triphosphate, the end product of the pathway, is a potent feedback inhibitor. Also, the enzyme is activated by adenosine triphosphate. This inhibition by a pyrimidine and stimulation by a purine is one mechanism for achieving balance in the synthesis of nucleic acids.

ATCase has a molecular weight of 310,000 (3) and contains two functionally distinct types of polypeptide chains, regulatory (R) and catalytic (C) (2, 3). The first indication of the hexameric nature (R_6C_6) of ATCase occurred when the x-ray study (4) demonstrated the simultaneous presence of both three-fold and two-fold molecular symmetry, and accurate molecular weights of the R and C chains were determined (5, 6). It is firmly established that the molecular symmetry is D_3 (7). This hexameric nature has been amply confirmed in more recent studies (6, 8–10). There are four cysteines on each R chain (5, 11) and one cysteine on each C chain (11, 12). Reaction of the thiols of the R chain with mercurials (3) causes dissociation of ATCase into two catalytic subunits (C_3) and three regulatory subunits (R_2) (3, 5). The cysteine of each catalytic chain in the intact ATCase molecule is unusually unreactive toward conventional reagents such as mercurials, N-ethylmaleimide, iodoacetic acid, and others (13, 14). This cysteine is more reactive in isolated catalytic subunits; it reacts slowly with p-hydroxymercuribenzoate (11, 13) and with 5,5′-dithiobis-(2-nitrobenzoate) (13). These reactions inactivate C_3 units, although smaller neutral substituents at the C-chain thiol do not (14). Permanganate rapidly oxidizes the C-chain thiol in both isolated catalytic subunits (15) and intact enzyme (14), causing loss of catalytic activity.

In this paper we review the three-dimensional structure, including arrangements of subunits, from an electron density map of ATCase at 5.5 Å resolution (16, 17). The regulatory properties of an intermediate C_6R_4 in the dissociation of the enzyme C_6R_6 will be described (18, 19). Finally, we make a brief comparison of our new electron density map of the complex of ATCase with the allosteric effector cytidine triphosphate (CTP). Differences in electron density are described which are probably associated with the binding of CTP and with changes of the protein conformation near the active site (20).

*Abbreviations: ATCase, aspartate transcarbamylase; C, catalytic chain; R, regulatory chain; PHMB, p-hydroxymercuribenzoate; MNP, 2-chloromercuri-4-nitrophenol; ATP, adenosine triphosphate; CTP, cytidine triphosphate; TIF, tetraiodofluorescene; Tris, tris (hydroxymethyl) aminomethane; βME, β-mercaptoethanol; SDS, sodium dodecyl sulfate.

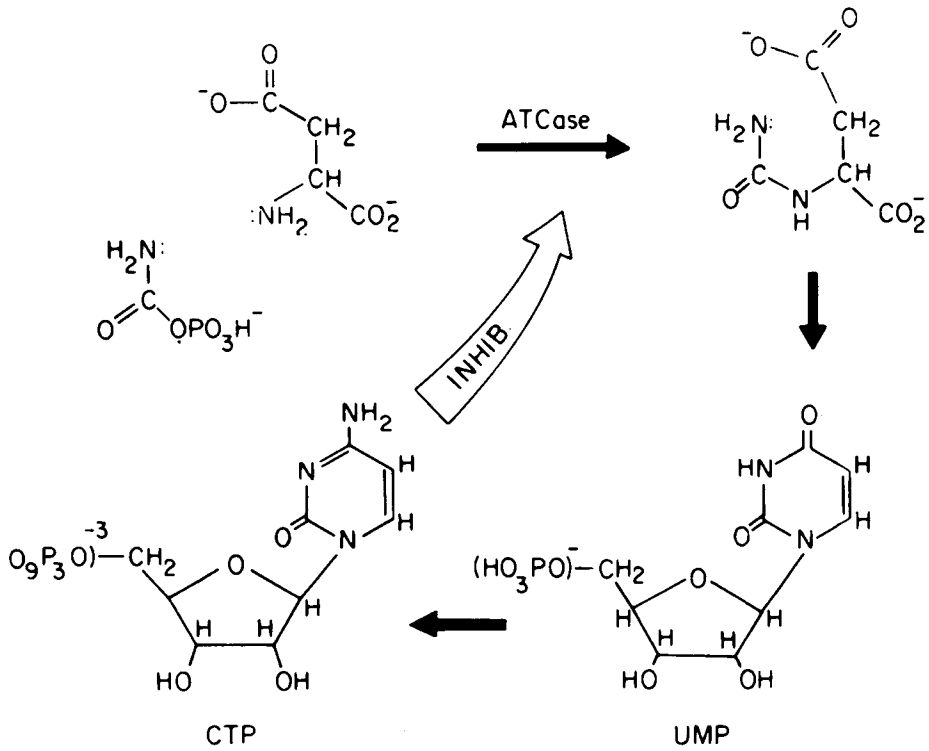

Fig. 1. ATCase catalyzes the reaction of carbamyl phosphate with aspartate to yield carbamyl aspartate and phosphate. This reaction is inhibited on a separate protein molecule of the enzyme complex by the end product of the pathway, cytidine triphosphate. ATP stimulates this enzymatic reaction.

ASPARTATE TRANSCARBAMYLASE AT 5.5 Å RESOLUTION

Solution of the three-dimensional structure depends upon the location of heavy atoms which then have known calculable contributions to the total scattering of protein plus heavy atoms. Comparison of these calculated contributions with the actual differences observed between magnitudes of scattering from the protein alone and the protein plus heavy atom then allows the phase of the x-ray scattering to be established for each reflection, relative to the origin chosen for the heavy atom in the unit cell of the crystalline protein. A review of this method is described elsewhere (21).

For large proteins, such as ATCase, the number of potential heavy atom sites becomes large and the scattering contribution of each heavy atom relative to that of the protein becomes small. For these reasons, we failed in all early attempts to locate multiple heavy atom sites obtained from immersion of crystalline protein in solutions of salts of heavy atom compounds. Only after a careful study of substitution at the relatively unreactive C-chain thiol were we able to obtain, for the first time, a reaction of this residue with a mercurial in the intact enzyme using the compound 2-chloromercuri-4-nitrophenol.

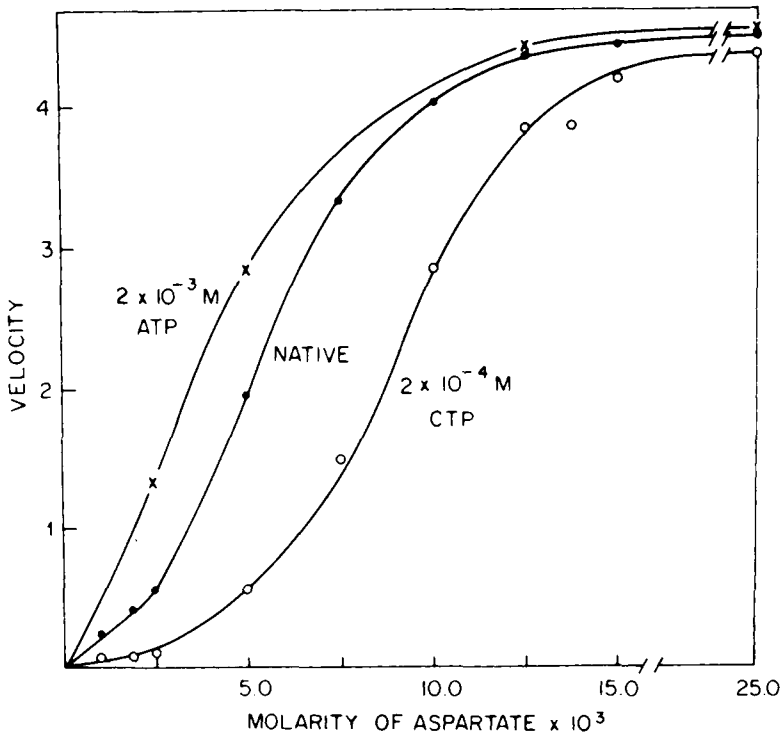

Fig. 2. Activity of ATCase as a function of aspartate concentration at saturating concentrations of carbamyl phosphate (native enzyme). The sigmoidal saturation curve is an indication of homotropic (cooperative) interaction between active sites. (From Gerhart, J. C. 1962. Ph.D. thesis, University of California, Berkeley.)

There is considerable evidence that C-chain thiol is in the vicinity of the active site (11, 13–15, 18, 22). Solution of the heavy atom in this derivative was the real break-through of the crystallographic part of this study, for it led quickly to the locations of first the major and then the minor sites of the much more complex heavy atom derivatives which we had previously not been able to solve.

Two crystal forms have now been solved to a resolution of 5.5 Å. The first is ATCase itself, in a form having space group R32 and hexagonal axes a = 131 Å and c = 200 Å (16). This crystalline form was obtained accidentally from a sample in an NMR tube being prepared for a kinetics experiment, under conditions which we felt sure would not lead to crystallization. One-sixth of the molecule is in the asymmetric part of the unit cell, the part not repeated by some symmetry operation. The molecular symmetry is thus D_3: a three-fold axis and three intersecting two-fold axes all perpendicular to the three-fold axis (Fig. 3).

The second form is the complex of ATCase with CTP. Here one-third of the molecule is in the asymmetric unit, and the molecular symmetry is required only to be C_3 (Schoenflies symbol). Thus one set of three-fold sites need not be equivalent to the other

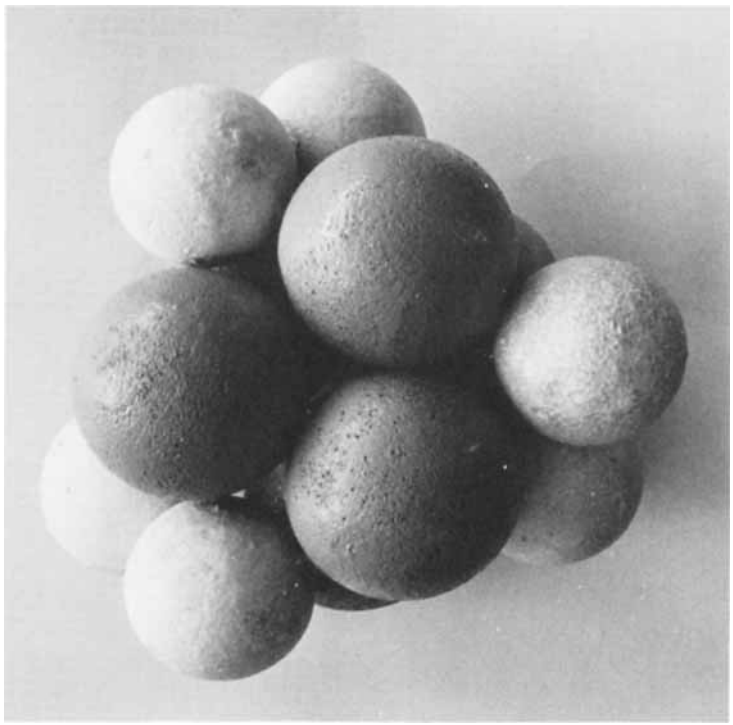

Fig. 3. Subunit structure of ATCase of symmetry D_3. The triangle of three larger balls represents one catalytic trimer (C_3). Another catalytic trimer is beneath this one, nearly eclipsed in this view along the molecular three-fold axis. Two-fold axes pass along directions from the center of the molecule through the point of contact of each pair R_2 of smaller balls. In the intermediate C_6R_4 described in Figs. 8–12 and 14 one regulatory pair R_2 is missing.

set in this crystal form. However, equivalence of all six sites is permitted even though not required. Discussion of this form, the ATCase-CTP complex (20), will be deferred until the final part of this article. We now return to the ATCase structure itself.

The complete electron density, which yields the model shown in Fig. 3, is given elsewhere (16). In the sections shown in Fig. 4, the density extends from a plane containing the molecular two-fold axes to about 21 Å through the molecule, toward the reader. The outer periphery of the triangle thus shows about half of the total electron density associated with the regulatory dimers, near the location of I: three of the six equivalent sites for the iodine atom of iodo-CTP. The denser region of density nearer the center, and including about half of the area of molecular density, is part of the catalytic trimer. This part contains the three Hg sites bonded to the C-chain thiols, and effectively covers the central cavity of the enzyme (Fig. 5). This cavity is, of course, also covered on the side away from the reader by the other catalytic trimer, consistent with the molecular symmetry of D_3. Aside from this large central aqueous cavity, the major features at this resolution are α-helices. Present estimates of about 35% in the C chain (MW 34,000) and

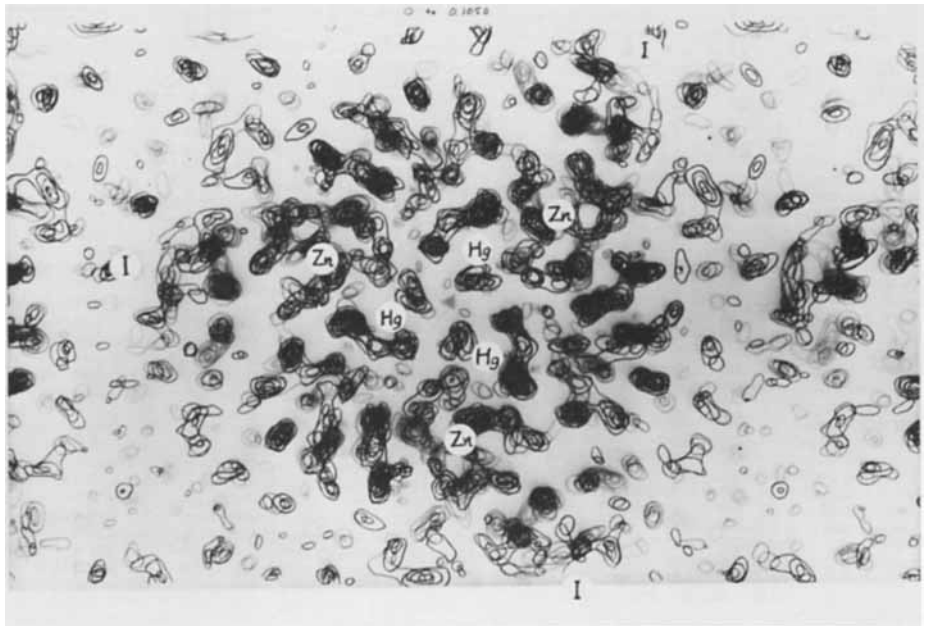

Fig. 4. Electron density of ATCase (R32 form) showing sections 0 – 0.1050 from the molecular center about halfway through the molecule along its three-fold axis. Positions are indicated for Hg (z = 0.1050 very near the active site), I (of iodo-CTP, z = 0.055, near the regulatory chain), and Zn (in the regulatory chain, z = 0.055, probably near the R:C interface). These values of z are 21 Å (for z = 0.1050) and 11 Å (for z = 0.055) above and below a plane containing the molecular two-fold axes. The weak electron density outside of the large triangle is due to aqueous solution in the crystal, except for larger densities at the extreme right and left associated with other molecules in the crystal.

about 10% in the R chain (MW 17,000) will possibly rise a bit as the resolution improves in later studies. A schematic view of the ATCase molecule, exploded along the three-fold axis in order to show the central cavity, is shown in Fig. 6.

An interesting feature is that the six active sites face the central cavity, not the outside of the ATCase molecule (Fig. 6). The most obvious access to this central cavity consists of six symmetry related access channels, about 15 Å in diameter in regions near the equatorial belt of the molecule (Fig. 7). The question then arises: What is the significance of these unexpected structural features and are they related to the regulatory properties of ATCase.

PROPERTIES OF THE INTERMEDIATE, C_6R_4

In studies on the modification of the C-chain thiol (18) we observed in 1972 that reaction of ATCase with small amounts of certain mercurials resulted in the formation of

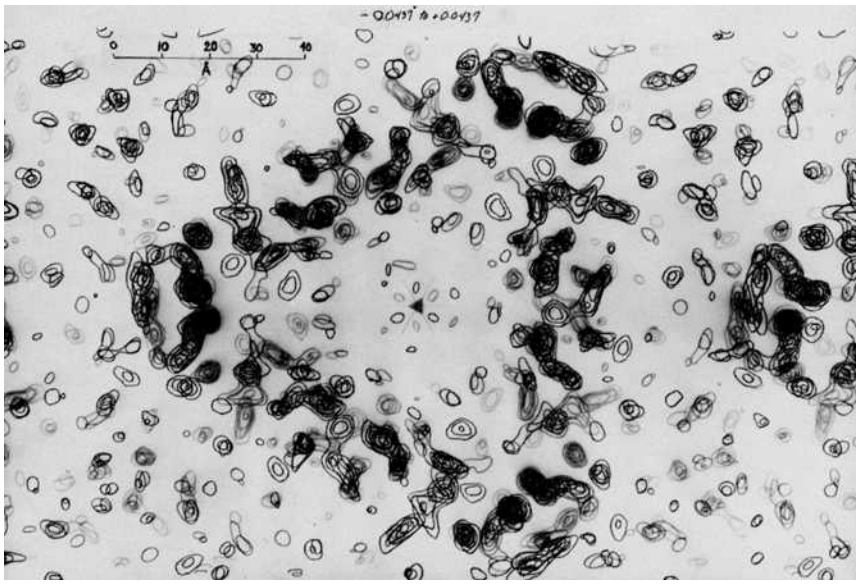

Fig. 5. Composite of 11 sections of electron density from z = −0.0437 to 0.0437, of the ATCase molecule. The central aqueous cavity has dimensions of about 50 Å along the two-fold axes in the plane of the map, and about 25 Å along the three-fold axis perpendicular to the plane of this map. Most of the regulatory protein lies in the outer corners of this large central triangle of electron density. Outside of the molecular density there is aqueous solution, except for a small part of a neighboring molecule at the right.

a protein, which we suspected was an intermediate in the dissociation of ATCase. At that time we began an investigation of this species and have shown (19) that it has a subunit of structure C_6R_4 and considerably altered regulatory properties. Schachman and coworkers in studies conducted at the same time on the assembly of ATCase (23) have independently characterized this species. This work, discussed by Schachman at the Ninth International Congress of Biochemistry (Stockholm, July 1–7, 1973), is also described in these proceedings. Also independently, Jacobson and Stark (14) have reported properties of an intermediate deficient in regulatory protein.

Partial dissociation of ATCase with the mercurial PHMB yields four components (ATCase, C subunit, R subunits, and intermediate) which can be resolved by cellulose acetate electrophoresis (Fig. 8). The intermediate, which can be isolated by DEAE sephadex chromatography, can react further with PHMB to yield $2C_3$ and $2R_2$, or can be reconverted to ATCase by addition of R_2 in the presence of Zn^{+2} and βME (Fig. 8). The composition C_6R_4 has been established from a molecular weight of 270,000 by gel filtration, and from C/R ratios established by sucrose gradient ultracentrifugation (Fig. 9), by cellulose acetate electrophoresis and by SDS electrophoresis. These experiments are summarized in Table I.

Titration of the intermediate, C_6R_4, with R_2 in the presence of Zn^{+2} yields

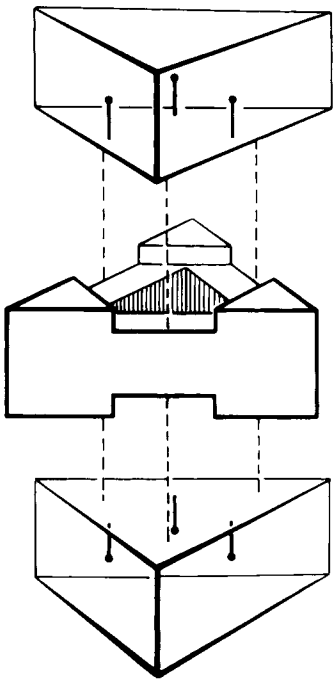

Fig. 6. Schematic view of the ATCase modecule expanded along the three-fold axis. This drawing does not indicate the mode of assembly, The central region is mostly composed of the three regulatory dimers. However, some parts of this region near ends of dotted lines may belong to the two catalytic trimers, which are drawn above and below this central region. The assembled molecule is about 90 Å along the three-fold axis and 110 Å along the two-fold axes. The central cavity (shaded) is about 25 Å along the three-fold axis and 50 Å along two-fold axes. Whithin the catalytic trimers Hg sites, near the active sites, are shown by dots joined by lines which indicate direct access toward the central cavity.

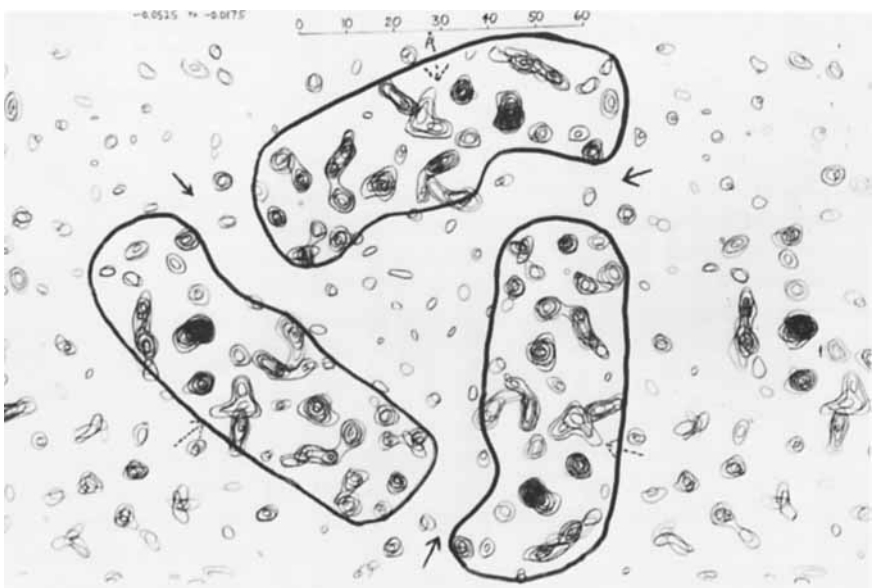

Fig. 7. Five sections of electron density of ATCase from z = −0.0525 to −0.0175, showing three (solid arrows) of the six access channels about 15 Å in diameter leading from the outer solution to the central cavity. The other three channels (dotted arrows) are in sections z = 0.0525 to 0.0175, related to these three by the D_3 symmetry of the ATCase molecule.

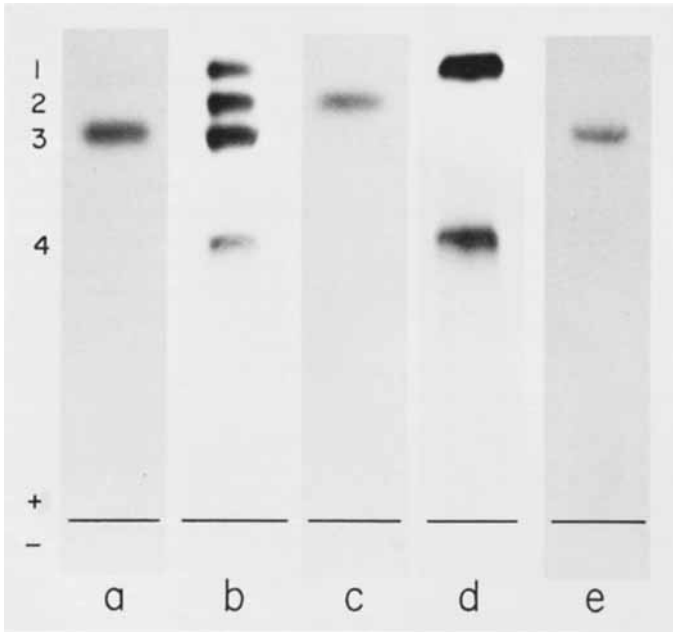

Fig. 8. Cellulose acetate electrophoresis of C_6R_6 (ATCase) and intermediate (C_6R_4), in 0.05 M Tris citrate at pH 7.8: a) R_6C_6; b) result of reaction of ATCase with 6 equivalents of PHMB, showing in order of decreasing mobility (1) C_3, (2) C_6R_4, (3) C_6R_6, and (4) R_2; c) Purified C_6R_4; d) result of reaction of C_6R_4 with a 50-fold molar excess of PHMB; e) purified C_6R_4 after incubation at 37° for 1 hr with a slight excess of ZnR_2, and 2×10^{-3} M βME. Staining and scanning procedures have been described elsewhere.

ATCase, and requires one mole of R_2 per mole of C_6R_4 (Fig. 10). For comparison we show that a similar titration of catalytic trimer also yields ATCase, but requires three moles of R_2 per two moles of C_3 (Fig. 10). The titration of the intermediate confirms the subunit structure, C_6R_4. Furthermore, the complete reconstitution of the native enzyme on the addition of one equivalent of regulatory subunit is a good indication that the intermediate is not an artifact resulting from some irreversible alteration of the molecule. The proportions of intermediate C_6R_4 produced when various molar ratios of PHMB react with ATCase are shown in Fig. 11.

The catalytic activities of ATCase, intermediate, and catalytic trimer are compared in Fig. 12 and Table I. In the absence of CTP or ATP the specific activities of C_6R_6 and C_6R_4 are essentially the same at saturating concentrations of carbamyl phosphate and 30 mM aspartate. At lower concentrations of aspartate (and at saturating carbamyl phosphate) the curve for the intermediate is still sigmoidal, although definitely less so than that for ATCase itself (at pH 8.3). This homotropic effect is summarized by the Hill coefficients of 3.3 for ATCase, but only 2.1 for the intermediate at pH 8.3. The residual cooperativity exhibited by the intermediate is apparent when its substrate saturation curve is compared with that of the catalytic subunit.

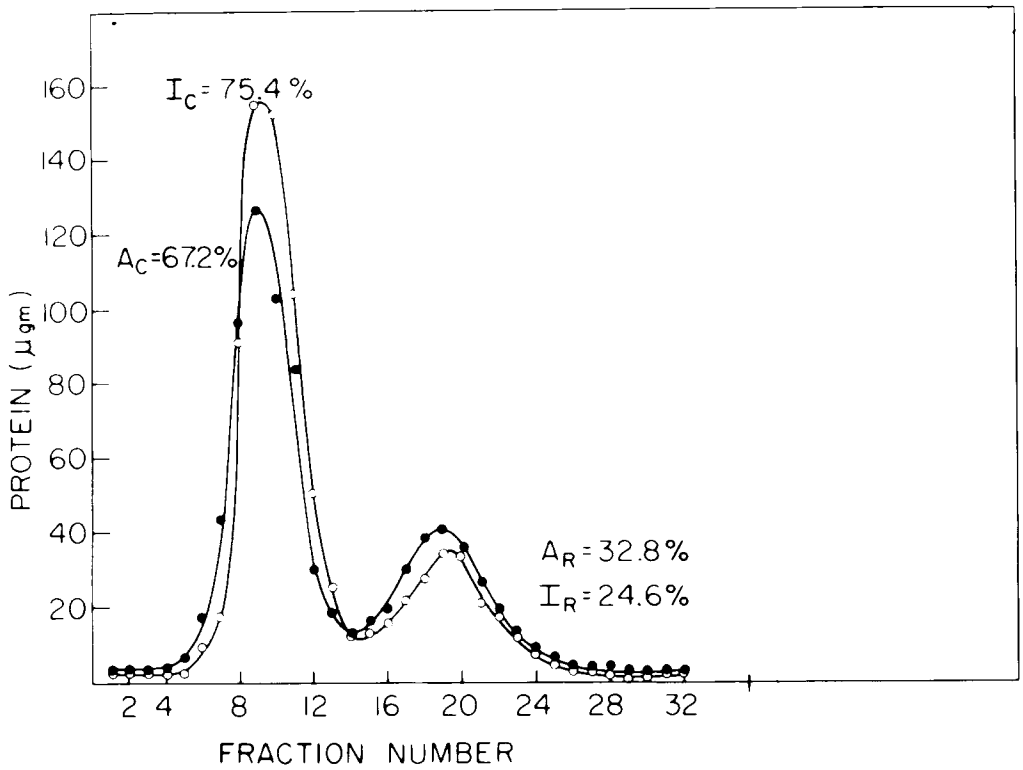

Fig. 9. Sucrose gradient (5–25%) ultracentrifuge fractionation after reaction of C_6R_6 (A) or C_6R_4 (I) with excess PHMB at pH 9.0. The partitioning into C_3's and R_2's is indicated, respectively, by subscripts C and R on A (ATCase) or I (Intermediate). The gradient was 5 to 25% sucrose, and the sample was spun for 16 hr at 45,000 Rpm.

Similarly the heterotropic effects (Table I) of the inhibitor CTP and the activator ATP are substantially reduced, but not abolished. At half saturating aspartate there is a decrease in percent inhibition by CTP from 59 in ATCase to 31 in the intermediate, while the percent stimulation by ATP decreases from 78 in ATCase to 26 in the intermediate.

The preservation of substantial homotropic and heterotropic interactions in the intermediate C_6R_4 indicates that the intact structure of ATCase is not required for these allosteric effects. It is therefore likely that access to the central cavity of the complete enzyme C_6R_6 does not play a dominant role in these regulatory processes.

In order to further correlate the properties of the intermediate with those of the isolated catalytic subunit and the native enzyme, we have employed tetraiodofluorescein (TIF, Fig. 13), a reagent which gives rise to opposite effects on the activities of the two enzyme forms (24).

Low concentrations of TIF increase native ATCase activity, while high concentrations decrease activity. In contrast, the catalytic subunit is inhibited by TIF at all con-

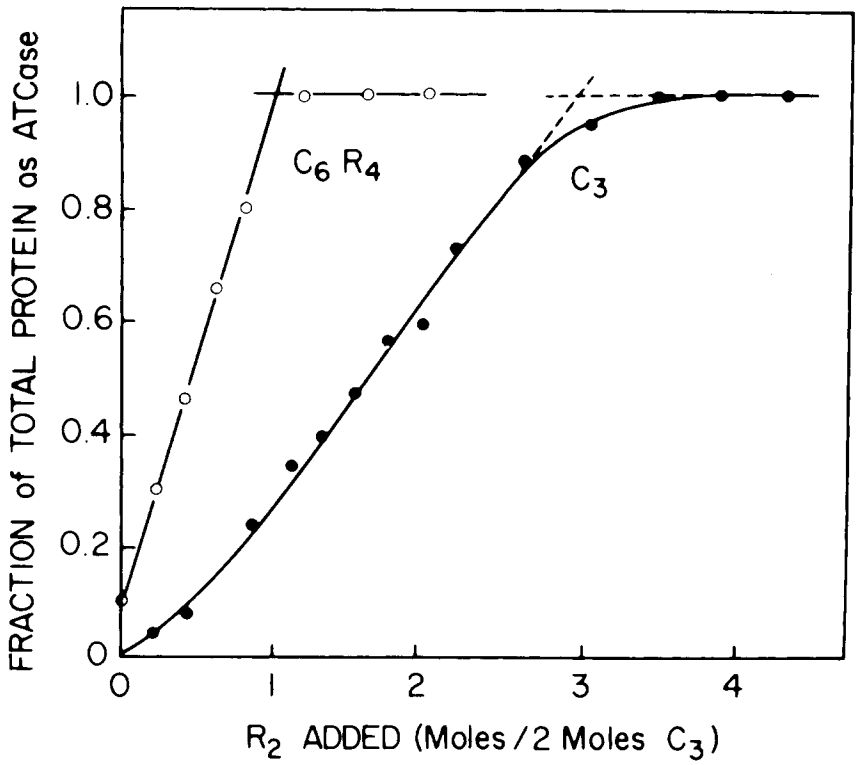

Fig. 10. Titration of the catalytic trimer and intermediate with regulatory dimer. Increasing amounts of ZnR_2 (3.0 mg/ml) were added to a series of reaction mixtures containing either 8.5 mg/ml intermediate or 9.2 mg/ml catalytic subunit in 0.05 M Tris HCl, pH 7.0. The samples were incubated in 2×10^{-3} M β mercaptoethanol for 30 min at 37°. Electrophoresis staining and scanning were carried out as described previously. The failure of the intermediate titration curve to intersect zero on the ordinate is an indication of a small amount of disproportionation ($3C_6R_4 \rightarrow 2C_3 + 2C_6R_6$) which occurred during storage, a process which would not be expected to alter the endpoint. Also, the initial curvature of the titration curve for C_3 reflects the formation, in the absence of mercurials, of a small amount of intermediate which is eventually titrated completely.

centrations. These results are interpreted to indicate at least two classes of binding site: an activating class on the regulatory subunits, corresponding to ATP sites, and an inhibiting class of sites on the catalytic subunit.

One possible explanation for these observations is that binding at the TIF site on the catalytic chain could be modified by the association of R chains to the catalytic trimers. When a regulatory dimer is removed from native ATCase, creating the intermediate, enough change is produced to alter substantially the binding or accessibility of TIF (Fig. 14). At low TIF concentrations, in contrast to native ATCase, intermediate is not activated to its ATP-stimulated level, while at higher TIF concentrations, in contrast to the catalytic subunit, intermediate is not completely deactivated.

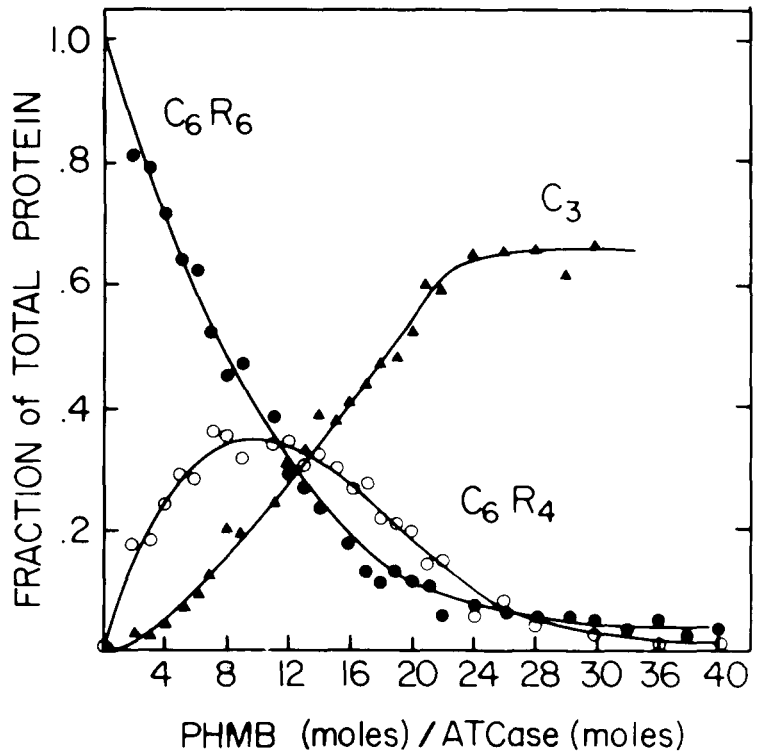

Fig. 11. The distribution of C_6R_6, C_6R_4, C_3 as a function of the molar ratio of PHMB/ATCase. The molar ratio of PHMB to ATCase was varied in a series of reaction mixtures (20 mg/ml ATCase in 0.05 M Tris Cl, pH 7.0). After the reaction had gone to completion the samples were spotted on cellulose acetate. Electrophoresis was carried out at 10 ma for 90 min using a 0.05 M phosphate pH 7.8 buffer system. The sheets were then stained in Ponceau S, destained with 5% acetic acid and cleared in Whitemor oil. The transparent sheets were pressed between glass plates and scanned using a Joyce Loebl double beam recording microdensitometer. The traces were integrated by planimetry. The data for R chain were not included since this method (cellulose acetate electrophoresis) gives erroneous values for R subunit at concentrations below about 2 mg/ml.

COMPARISONS OF ELECTRON DENSITIES AT 5.5 Å RESOLUTION OF ATCase, AND OF ITS COMPLEX WITH CTP

The electron density map of the ATCase-CTP complex has been solved to 5.5 Å resolution. To identify the nucleotide binding sites, the CTP bound within the crystal was exchanged with 5-iodo-CTP and the position of the iodine was then located by difference Fourier techniques. The principal nucleotide binding site is on the outer surface of the regulatory subunit (Fig. 4). A minor iodo-CTP site is also evident in the vicinity of the active site, as expected (26), but is not shown in the figure.

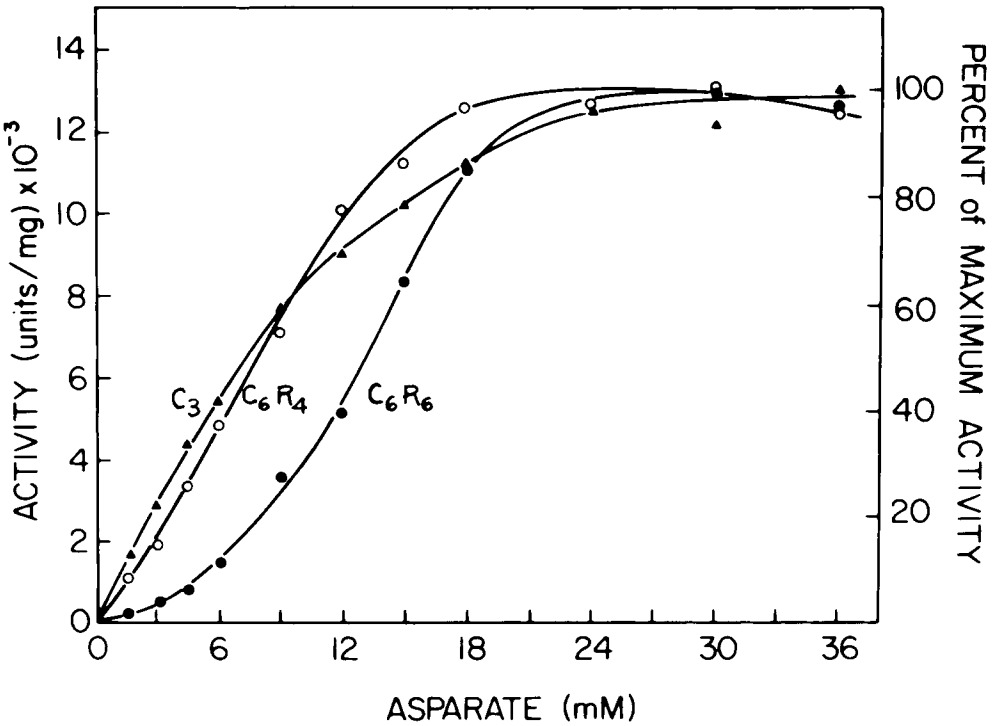

Fig. 12. Aspartate saturation curves of C_6R_4, (intermediate), C_6R_6 (ATCase), and C_3. Catalytic activity was measured by monitoring the release of protons at pH 8.3 using a radiometer TT2 pH stat. All assays were carried out at saturating (4.8 mM) levels of carbamyl phosphate. Activities for ATCase (●) and intermediate (○) are expressed in μ moles hr^{-1} mg^{-1}. The hyperbolic curve for the specific activity of C_3 (▲) has been renormalized (at 31 mM) so that shapes of these three curves may be readily compared. The actual specific activity of C_3 is 1.45 greater than that of C_6R_6 at saturating carbamyl phosphate and 30 mM aspartate. All of the species, C_3, C_6R_6, and C_6R_4, exhibit substrate inhibition at high concentrations of aspartate. For the catalytic subunit, accurate values for K_m and V_{max} can be obtained by extrapolating the double reciprocal plot, a procedure which is not applicable to C_6R_6 or C_6R_4 because of the nonlinearity of these plots. Consequently the reported values for the Hill coefficients (the calculation of which depends on V_{max}) may be considered only reasonable estimates and may actually be somewhat lower, while the values for K_m reported in Table I for C_6R_6 and C_6R_4 may be somewhat higher.

Electron densities at 5.5 Å resolution for ATCase (Fig. 15) and for CTP – ATCase (Fig. 16) show surprisingly similar electron densities. We caution that some of the differences of electron densities discussed here may be comparable with errors in the maps. The sets of sections in Figs. 15 and 16 have been selected as comparable regions of these two forms of the enzyme; they contain the active sites (black dots indicate the Hg position), and show extra density near the regulatory region which itself is below these sections (away from the reader). This extra density (1, Fig. 16) is very near the iodine site in iodo-CTP-ATCase. A shift of electron density appears near the active site (2, Fig. 16). Finally,

TABLE I. Comparison of C_6R_4 (Intermediate) and C_6R_6 (ATCase)

		Intermediate	ATCase
Wt. % catalytic		76[a], 75[b], 74[c] (75)[d]	67[a], 67[b], –, (67)[d]
Wt. % regulatory		24, 25, 26 (25)	34, 33, –, (34)
MW, gel filtration		270,000	310,000[e]
Formula		C_6R_4	C_6R_6
Thiols		22[f]	30
Spec. activity (μmoles/hr/mg)	pH 8.3	1.3×10^4	1.3×10^4
K_M (app.), aspartate (mM)	pH 8.3	9	13
Hill coeff. (homotropic)	pH 8.3	2.1	3.3
ATP (2 mM) % activation	pH 8.3	26	78
CTP (1 mM) % inhibition	pH 8.3	31	59

[a]Cellulose acetate electrophoresis (C_3,R_2)
[b]Sucrose gradient ultracentrifugation (C_3,R_2).
[c]SDS gel electrophoresis (C, R).
[d]Theoretical, from MW of C and R chains.
[e]Literature value (3, 6), by ultracentrifugation.
[f]Theoretical value; the measured value is 20, based on the PHMB method (Boyer, P. D., J. Amer. Chem. Soc. *74*, 4331).

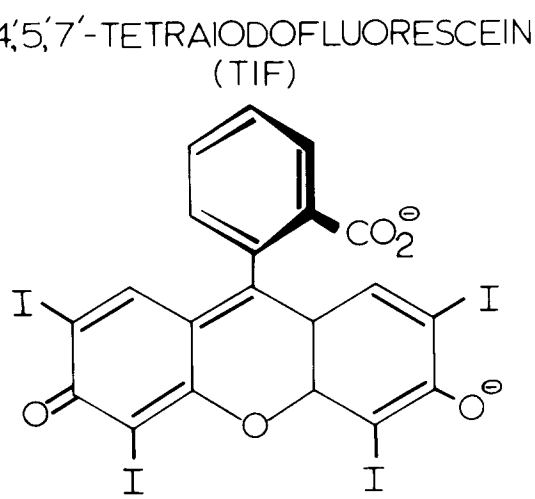

Fig. 13. Chemical formula of 2', 4', 5', 7' -tetraiodofluorescene (TIF).

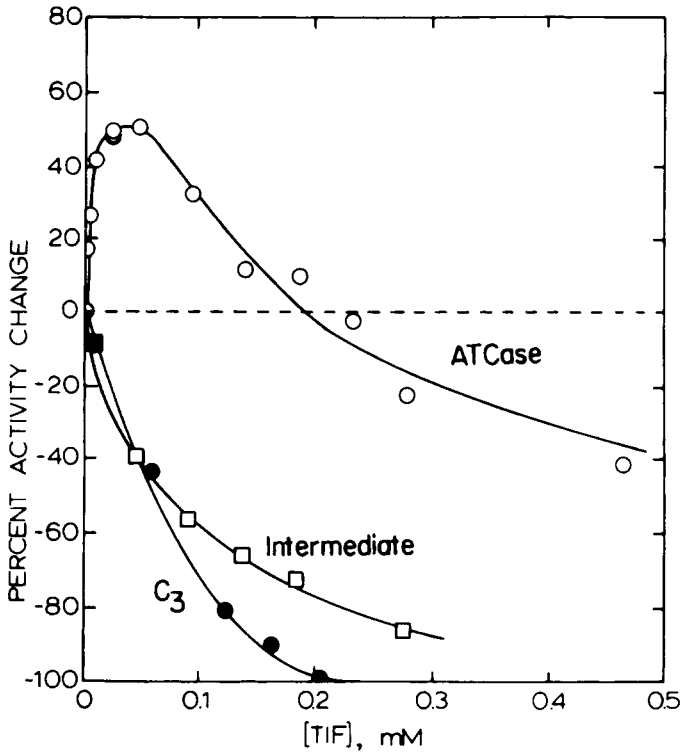

Fig. 14. Effect of increasing concentrations of TIF on C_6R_6, C_3, and C_6R_4. At low concentrations of TIF, ATCase is stimulated, but C_3 is inhibited. At these low concentrations TIF inhibits the intermediate.

there are other conformational differences in these sections (for example 3, Fig. 16) and elsewhere in the map. A detailed study of these differences is now under way. Also, these structures are being carried to high resolution (2.8 or 3.0 Å). It does seem likely that conformational changes are propagated through the enzyme structure from the effector (CTP or ATP) site to the active site region, a distance of about 55 Å.

At least an additional three-dimensional structure is required in order to understand other conformational changes induced in ATCase when inhibitors (e.g., succinate) or product analogues (e.g., N-phosphonacetyl-L-aspartate) are bound. This latter compound, PALA, which has been shown by Collins and Stark (25) to shift the enzyme into the activated conformation, yields crystals of space group R32, having unit cell dimensions of a = 122 Å and c = 701 Å. The asymmetric unit contains one-half of the ATCase molecule. This structure is also under investigation.

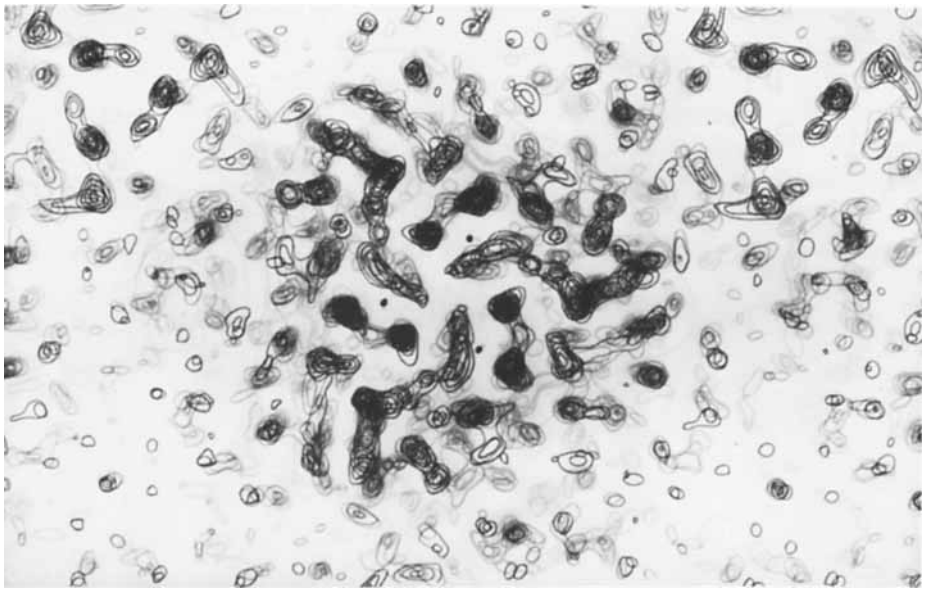

Fig. 15. Composite electron density map of ATCase including primarily the region of the catalytic trimer. The black dots indicate the position of mercury attached to the catalytic sulfhydryl group.

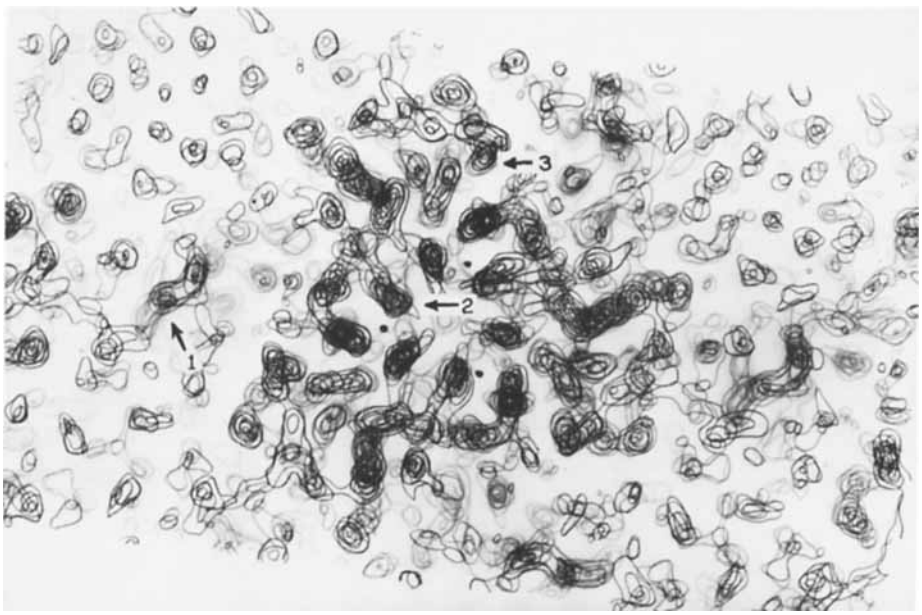

Fig. 16. Composite density map of the complex of ATCase with CTP showing the sections corresponding to those in Fig. 15 for ATCase. Regions of added or modified density are indicated by arrows: 1. extra density near regulatory regions; 2. shift of density near catalytic regions; 3. other modified density in these regions of the molecule. Six CTP molecules are bound per ATCase molecule.

ACKNOWLEDGMENT

This research was supported by the National Institutes of Health, Grant GM 06920. We wish to thank L. B. Jacobsberg and E. R. Kantrowitz for unpublished studies of the interaction of TIF with ATCase, and G. Eisele and S. Landfear for the location of iodo-CTP in the ATCase molecule.

REFERENCES

1. Yates, R. A., and Pardee, A. B., J. Biol. Chem. 221:757 (1956).
2. Gerhart, J. C., and Pardee, A. B., J. Biol. Chem. 237:891 (1962).
3. Gerhart, J. C., and Schachman, H. K., Biochemistry 4:1054 (1965).
4. Wiley, D. C., and Lipscomb, W. N., Nature 218:1119 (1968).
5. Weber, K., Nature 218:1116 (1968).
6. Rosenbusch, J. P., and Weber, K., J. Biol. Chem. 246:1644 (1971).
7. Wiley, D. C., Evans, D. R., Warren, S. G., McMurray, C. H., Edwards, B. F. P., Franks, W. A., and Lipscomb, W. N., Cold Spring Harbor Symp. Quant. Biol. 36:285 (1971).
8. Meighen, E. A., Pigiet, V., and Schachman, H. K., Proc. Nat. Acad. Sci. U.S. 65:234 (1970).
9. Richards, K. E., and Williams, R. C., Biochemistry 11:3393 (1972).
10. Cohlberg, J. A., Pigiet, Jr., V. P., and Schachman, H. K., Biochemistry 11:3396 (1972).
11. Gerhart, J. C., and Schachman, H. K., Biochemistry 7:538 (1968).
12. Weber, K., J. Biol. Chem. 243:543 (1968).
13. Vanaman, T. C., and Stark, G. R., J. Biol. Chem. 245:3565 (1970).
14. Jacobson, G. R., and Stark, G. R., J. Biol. Chem. 248:8003, 8014 (1973).
15. Benisek, W. F., J. Biol. Chem. 246:3151 (1971).
16. Warren, S. G., Edwards, B. F. P., Evans, D. R., Wiley, D. C., and Lipscomb, W. N., Proc. Nat. Acad. Sci. U.S. 70:1117 (1973).
17. Evans, D. R., Warren, S. G., Edwards, B. F. P., McMurray, C. H., Bethge, P. H., Wiley, D. C., and Lipscomb, W. N., Science 179:683 (1973).
18. Evans, D. R., McMurray, C. H., and Lipscomb, W. N., Proc. Nat. Acad. Sci. U.S. 69:3638 (1972).
19. Evans, D. R., Pastra-Landis, S. C., and Lipscomb, W. N., Proc. Nat. Acad. Sci. U.S. 71:1351 (1974).
20. Edwards, B. F. P., Evans, D. R., and Lipscomb, W. N., Proc. Nat. Acad. Sci. U.S. to be published; also B. F. P. Edwards, Ph.D. thesis, Harvard University, 1974.
21. Jacobson, R. A. and Lipscomb, W. N., in "Physical Methods of Chemistry," Vol. 1, Part IIID, (A. Weissberger and B. W. Rossiter, Eds.), p. 1. John Wiley and Sons, New York (1972).
22. McMurray, C., Evans, D. R., and Sykes, B., Biochem. Biophys. Research Commun. 48:572 (1972).
23. Yang, Y. R., Syvanen, M., Nagel, G., and Schachman, H. K., Proc. Nat. Acad. Sci. U.S. 71:918 (1974).
24. Jacobsberg, L. B., Kantrowitz, E. R., McMurray, C. H., and Lipscomb, W. N., Biophys. Biochem. Res. Commun. 55:1255 (1973).
25. Collins, K. D., Stark, G. R., J. Biol. Chem. 247:6599 (1971).
26. Porter, R. W., Modebe, M. O., and Stark, G. R., J. Biol. Chem. 244:1846 (1969).